ACS APPLIED MATERIALS & INTERFACES

Research Article

www.acsami.org

Solution-Processed and Air-Stable n-Type Organic Thin-Film Transistors Based on Thiophene-Fused Dicyanoquinonediimine (DCNQI) Deriatives

Shiyan Chen,*[,†] Yan Zhao,[‡] Altan Bolag,[§] Jun-ichi Nishida,[§] Yunqi Liu,[‡] and Yoshiro Yamashita*[,§]

[†]State Key Laboratory for Modification of Chemical Fibers and Polymer Materials, Key Laboratory of Textile Science & Technology (Ministry of Education), College of Materials Science and Engineering, Donghua University, Shanghai 201620, P.R. China

[‡]Beijing National Laboratory for Molecular Sciences, Key Laboratory of Organic Solids, Institute of Chemistry, Chinese Academy of Sciences (CAS), Beijing 100190, China

[§]Department of Electronic Chemistry, Interdisciplinary Graduate School of Science and Engineering, Tokyo Institute of Technology, Nagatsuta, Midori-ku, Yokohama 226-8502, Japan.

Supporting Information

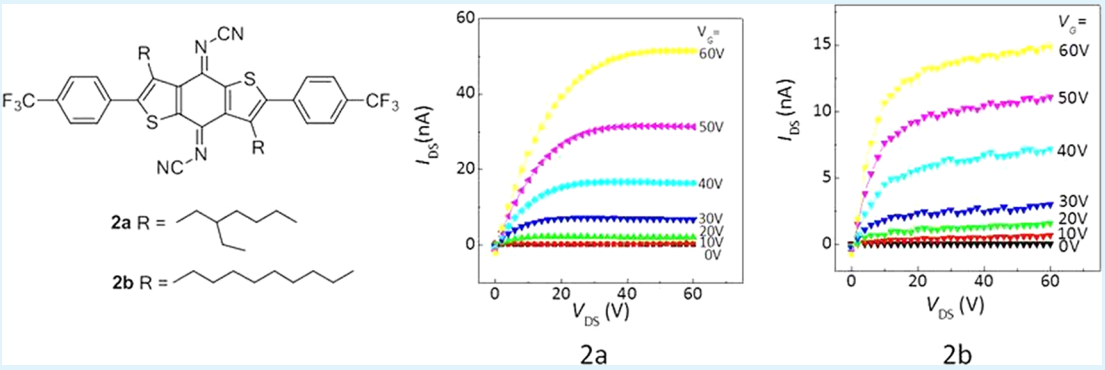

ABSTRACT: π-Conjugated systems **2a** and **2b** containing thiophene-fused DCNQI with long alkyl and trifluoromethylphenyl groups were synthesized as potential active materials for solution-processed and air-stable n-type organic thin-film transistors (OTFTs). The electrochemical measurements revealed that the lowest unoccupied molecular orbital (LUMO) of the compounds have an energy level less than −4.0 eV, indicating air stable n-type materials. The long alkyl groups endowed the compounds good solubility and solution-processability. X-ray diffraction measurements revealed the difference of the molecular arrangement depending on the alkyl groups, which were also observed in the UV−vis absorptions of the films. A relatively good mobility up to 0.003 $cm^2\ V^{-1}\ s^{-1}$ for **2a** by spin-coating was obtained with good air stability.

KEYWORDS: *thiophene-fused DCNQI, n-type, solution-processed, air-stable, organic thin-film transistors*

INTRODUCTION

Organic thin-film transistors (OTFTs) have been attracting attention because of their potential as low-cost, large-area, and flexible organic electronic devices.[1−6] So far, the most devices with high performances were fabricated by vacuum process which requires high vacuum and high temperature. To realize the low-cost, convenient, and large-area organic electronics, solution techniques such as spin-coating, casting, or inkjet printing are required for devices fabrication. Second, the devices should have high mobility to provide sufficiently large drive current in the circuits. Moreover, stable operation in air is very important for practical applications. To date, some solution-processed p-channel OTFTs have shown hole mobilities more than 1.0 $cm^2\ V^{-1}\ s^{-1}$ with good air stability.[7−11]

Great progress in solution-processed, n-type OTFTs in ambient conditions has been made in recent years, such as Zhu et al. reporting dicyanomethylene-substituted fused tetrathienoquinoid[12−14] with the electron mobility as high as 0.9 $cm^2\ V^{-1}\ s^{-1}$ and observing dicyanomethylene-substituted fused tetrathienoquinoid[15] with the electron mobility as high as 1.2 $cm^2\ V^{-1}\ s^{-1}$. Marder et al. also reported bis(naphthalene diimide) derivatives as the solution-processed n-channel OTFTs with the high electron mobility of 1.5 $cm^2\ V^{-1}\ s^{-1}$.[16] Some n-channel OTFTs based on polymers are also reported with the electron mobility near 1.0 $cm^2\ V^{-1}\ s^{-1}$.[17] The representative example is an OTFT based on an electron transfer copolymer of naphthalene-bis(dicarboximide)(NDI) and bithiophene with the highest mobility of 0.85 reported by Facchetti et al..[18] However, compared to the high performances of p-channel OTFTs, solution-processed n-channel OTFTs are

Received: May 10, 2012
Accepted: July 30, 2012
Published: July 30, 2012

Scheme 1. Synthetic Route to Compounds 2a and 2b[a]

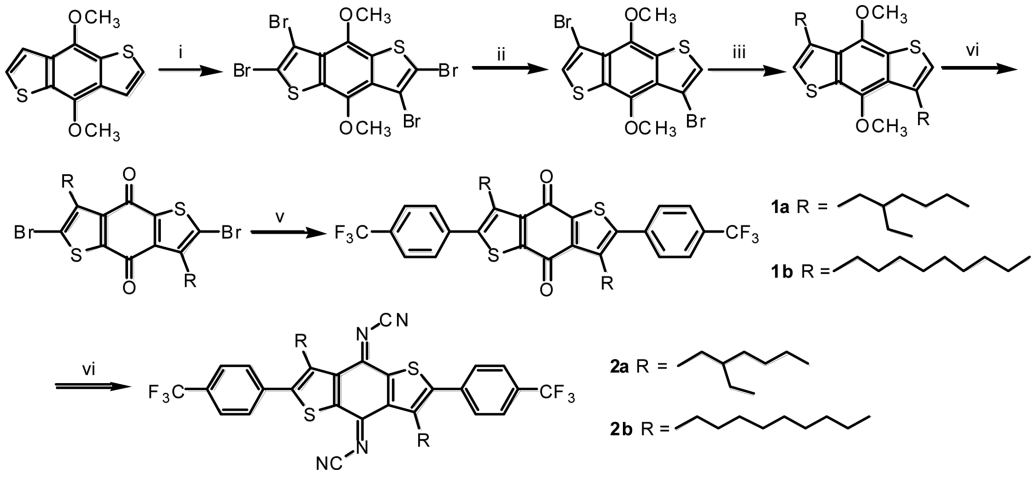

[a]Reagents and conditions: (i) Br_2, CS_2, reflux, 24h, 95%. (ii) CH_3COOH, Zn, reflux, 2h, 80%. (iii) RMgBr, [$NiCl_2$(dppp)], Et_2O, reflux, 12h, 85%. (vi) Br_2, CH_2Cl_2, rt, 2h, 94%. (v) cat, $Pd(PPh_3)_4$, THF, K_2CO_3 (1 M aq), reflux, 24 h, 91%. (vi) $Me_3SiNCNSiMe_3$, $TiCl_4/CHCl_3$, reflux, 12h, 96%. dppp = 1,3-bis(diphenylphosphanyl)propane.

still lags behind. The papers reported on n-type materials with good electron-transport characteristics, air-stability and good solution-processability suitable for the fabrication of OTFTs by solution deposition techniques are relatively rare.[17−21] Therefore, it is still a challenge to develop air-stable, solution-processable n-channel OTFTs.

Benzodithiophene is a very promising building block for organic electronics.[22] The benzodithiophene core can be functionized with electron-donating or electron-withdrawing functional groups to give a promising class of semiconductors suitable for n- or p-type OTFTs[23−27] and solar cells,[28−33] and some of them displayed promising device performances. To date, the highest electron mobility of trifluoromethylthiazoyl substituted benzodithiophene-4,8-dione was 0.15 $cm^2\ V^{-1}\ s^{-1}$. This result was reported by our group previously and the system is based on vacuum-deposited devices.[23] For solution processed OTFTs, only p-type OTFTs based on polymers have been reported and the highest mobility of 0.4 $cm^2\ V^{-1}\ s^{-1}$ was reported by Ong and co-workers.[24] However, solution-processed n-channel OTFTs based on benzodithiophene derivatives have not been reported so far. On the other hand, DCNQI-based compounds are famous as strong-electron acceptors and a few papers have been published for investigating their conducting properties. Compared with the classical acceptor TCNQ (tetracyanoquinodimethane), they overcame the steric drawbacks and opened a new route to organic conducting materials.[34] Thiophene-fused DCNQI compounds[35−37] and polymers[38] have also been reported. However, the materials based on the building block molecules for OTFT have not been reported. In this paper, two new thiophene-fused DCNQI with long alkyl and trifluoromethylphenyl groups were first synthesized and characterized. The OTFTs based on them were prepared by dip casting and spin-coating methods. The derivative **2a** showed good n-type OTFT behavior with a mobility more than 0.003 $cm^2\ V^{-1}\ s^{-1}$ and on/off of 1×10^5 in air.

RESULTS AND DISCUSSION

1. Synthesis and Thermal Properties. Scheme 1 presents the synthetic route to the target compounds **2a** and **2b**. First, 4,8-dimethoxybenzo[1,2-*b*:4,5-*b*′]dithiophene was brominated at the 2, 3, 6, and 7 positions to give a tetrabromo compound, where 10 equiv of bromine were used to ensure a complete reaction. Selective debromination of the tetrabromide at the 2 and 6 positions afforded 3,7-dibromo compound. The two alkyl groups were introduced at the 3 and 7 positions by the Grignard reaction. Then, bromination at the 2 and 6 positions with bromine in CH_2Cl_2 with simultaneous demethoxylation gave 2,6-dibromobenzo[1,2-*b*:4,5-*b*′]dithiophene-4,8-dione. The palladium-catalyzed Suzuki coupling reaction of the dibromide with 4-trifluoromethylphenylboronic acid afford the diones **1a** and **1b.** Then, the target compounds **2a** and **2b** were subsequently prepared in good to excellent yields (>90%) by the reaction of **1a** and **1b** with *N*,*N*-bis-(trimethylsilyl)carbodiimide (BTC) promoted by titanium tetrachloride (10 equiv) in refluxing chloroform according to previously published papers.[39] The obtained compounds were characterized by HNMR, MS, and elemental analyses. As expected, **2a** and **2b** are highly soluble in solvents such as chloroform, tetrahydrofuran, and chlorobenzene (>10 mg/mL). The good solubility endows them to fabricate devices with solution processing. The thermal properties of **2a** and **2b** were investigated by DSC measurements. They exhibited the melting points at 154 and 206 °C, respectively. The obvious difference can be attributed to the effect of long alkyl groups affecting the molecular arrangement in the solid state which will be discussed in the following section.

2. Optical and Electrochemical Properties. The optical properties of the molecules were examined by UV−vis spectroscopy in CH_2Cl_2 solution and in the films. The data are summarized in Table 1. As shown in Figure 1, the spectrum of **2a** in solution is almost the same as that of **2b**,

Table 1. Optical and Electrochemical Data of 2a and 2b

	λ^{abs}max (nm)					
compd	solution	film	band gap (eV)	$E_{1/2}^{red}$ (V)	HOMO (eV)	LUMO (eV)
2a	291, 372, 388, 450	292, 390	2.15	−0.12, −0.63	−6.37	−4.22
2b	291, 372, 388, 449	277, 440	2.15	−0.17, −0.71	−6.32	−4.17

dx.doi.org/10.1021/am300822z | ACS Appl. Mater. Interfaces 2012, 4, 3994−4000

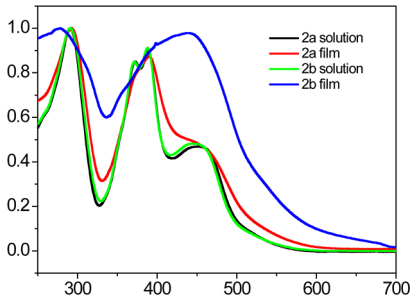

Figure 1. Normalized electronic absorption spectra of **2a** and **2b** in CH_2Cl_2 solution and in the films.

demonstrating that the different long alkyl units have no obvious effect on the absorptions. However, significant differences of absorptions are seen in the films. Thus, for **2a**, compared with that in solution, only a little red shift was observed in the film implying no strong intermolecular interaction in the film, whereas, for **2b**, the fine absorptions in solution disappeared and instead, a broad absorption band was observed in the solid state, suggesting the formation of aggregates.[40−42] Moreover, an obviously red shift was also observed, indicating that the molecular arrangement in the films is different form that in solution and a strong intermolecular interaction exists in the films. This result indicates that the substituents grafted on the benzo[1,2-*b*:4,5-*b*′]dithiophene core can affect the intermolecular interactions in the solid state, which are important to control their charge transport properties.

A further insight into the electronic properties of **2a** and **2b** was given by cyclic voltammetry. Figure 2 shows the reduction

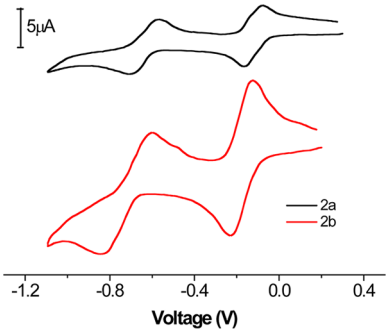

Figure 2. Cyclic voltammograms of **2a** and **2b** in 0.1 M Bu_4NPF_6−CH_2Cl_2, scan rate 100 mV s^{-1}.

waves of **2a** and **2b** and the data are listed in Table 1. They both exhibited reversible stepwise reduction couples, suggesting that they have good electron transport properties. The reduction potentials of **2a** and **2b** are almost the same, indicating that the LUMO levels are not largely affected by the long alkyl substituents. Their energy levels were calculated using the ferrocene (E_{FOC}) value of −4.8 eV as a standard, while the E_{FOC} was calibrated to be 0.46 V vs SCE in a ferrocene CH_2Cl_2 solution. The electron affinity (EA) (LUMO level) for **2a** and **2b** derived from the first half-wave reduction potentials (EA = ($E_{1/2}^{red\text{-}1}$ + 4.34) are −4.22 and −4.17 eV, respectively. These values are lower than −4.0 eV, which is the LUMO level to be required for air-stable n-channel OTFTs.[43−46]

3. OTFT Characteristics. The OTFT devices were fabricated with bottom-contact configuration. The organic semiconductors were deposited by dip casting and spin-coating methods. Device fabrication and measurement details are given in the Experimental Section. The OTFT devices based on compounds **2a** and **2b** were first fabricated by dip casting 1 mg/mL chloroform solutions. Typical n-type organic semiconductor characteristics were observed and the OTFT performances of the devices are summarized in Table 2. The **2a** and **2b** OTFTs fabricated by a dip casting method on the bare substrate in air exhibited field-effect electron mobilities of 2.71×10^{-7} and 4.61×10^{-6} cm^2 V^{-1} s^{-1} for threshold voltages of −2 and 0 V, respectively. Several devices based on the method had been tested and the order of magnitude for the obtained field-effect electron mobilities was in the same. In these devices the semiconductor films were irregular and discontinuous, leading to the low OTFT performances. For **2b**, the OTFT mobility is one order magnitude higher than that of **2a**, probably because of the different molecular arrangement and film morphorogy. In order to improve the film morphology and the OTFT performances, spin-coating followed by thermal annealing was carried out. Thus, the semiconductor layer was deposited on the OTS-treated Si/SiO_2 substrates by spin-coating of chloroform solution (10 mg/mL). Representative output and transfer characteristics of devices fabricated with **2a** and **2b** by spin-coating method are shown in Figure 3 and the OTFT data are summarized in Table 2. The highest electron mobility of **2a** on the OTS-treated substrate by the spin-coating method in air reached around 0.003 $cm^2V^{-1}s^{-1}$, which is increased 4 orders of magnitude compared with the dip casting method. For **2b**, the highest electron mobility also increased by 2 orders of magnitude over the dip casting. Although the OTFT performances increased obviously both for **2a** and **2b** by spin-coating method compared with the dip-casting method, the electron mobilities for **2a** are higher than those of **2b.** It is opposite to the results from the dip-casting method. The phenomenon may be explained that the crystallinity of **2b** is better than that of **2a** at room temperature, which is confirmed by the XRD results of the film by dip-casting method. However, when the film formed by spin-coating method and annealed at 120 °C, the crystallinity of **2a** was improved obviously and the crystalline grain of **2a** is larger than that of **2b** (confirmed by the following XRD and AFM results). So large grain boundaries

Table 2. Field-Effect Transistor Characteristics of Bottom-Contact Devices for 2a and 2b in Air[a]

compd	substrate conditions	deposition method	T (°C)	μ (cm^2 V^{-1} s^{-1})	I_{on}/I_{off}	V_{th}(V)
2a	bare[b]	dip casting	25	2.71×10^{-7}	1×10^2	−2
	OTS-treated[c]	spin-coating	annealed at 120 °C	$3.01(1.75) \times 10^{-3}$	1×10^5	7
2b	bare[b]	dip casting	25	4.61×10^{-6}	1×10^2	0
	OTS-treated[c]	spin-coating	annealed at 120 °C	$5.04(2.97) \times 10^{-4}$	1×10^4	9

[a]Numbers in brackets show the average mobilities for the devices. [b]SiO_2: 300 nm, L/W = 25 μm/294000 μm, S/D electrode: Au/Cr (20/10 nm). [c]SiO_2: 300 nm, L/W = 10 μm/1400 μm, S/D electrode: Au (30 nm).

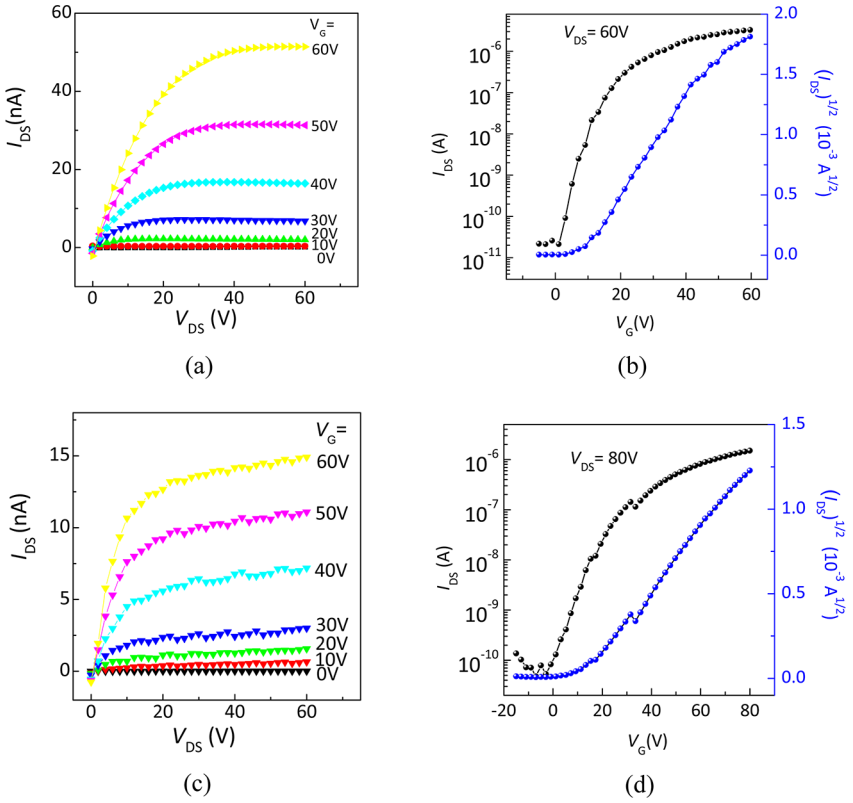

Figure 3. Representative (a) output and (b) transfer characteristics for **2a**, (c) output and (d) transfer characteristics for **2b** on the OTS-treated SiO_2 substrate annealed at 120 °C.

exist in the **2b** film are more than those in **2a** film which leads to the lower electron mobilities of **2b** than those of **2a**. The results also demonstrate that these molecules are promising n-type semiconductors for organic OTFTs and the OTFT performances are strongly dependent on the solution processing conditions. Furthermore, to investigate the air-stability, the devices based on **2a** and **2b** were stored in air, and the OTFT characteristics were measured periodically. As shown in Figure 4, the electron mobility of 1×10^{-3} cm^2 V^{-1} s^{-1} for **2a**

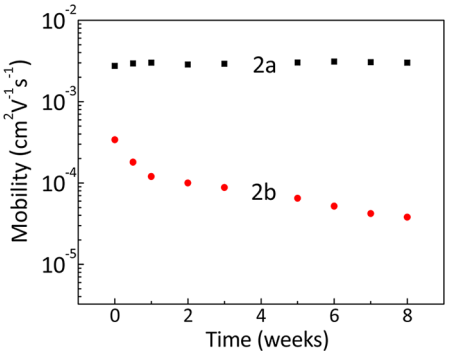

Figure 4. Electron mobility of OTFTs based on **2a** and **2b** versus storage period.

was kept over a period of 8 weeks. The excellent air stability of the device for **2a** is attributed to the combination of the low-lying LUMO level (−4.22 eV) of the organic semiconductor and its good crystallinity (confirmed by the AFM and XRD characterization in the following sections), both of which prevent the trapping of electron carriers and the intrusion of oxygen and/or moisture. On the other hand, the mobility for **2b** decreased by 1 order of magnitude after storage in air for 8 weeks. Because **2b** has the similar low-lying LUMO level (−4.17 eV), the film of **2b** might be less crystallinity due to the unfavorable molecular arrangement, which leads to the decrease in its mobility.

4. Surface Morphology Analysis. Macroscopic images and atomic force microscopy (AFM) were recorded to examine the surface morphologies and the roughness of the spin-coating thin films. Figure 5 shows the macroscopic images of spin-

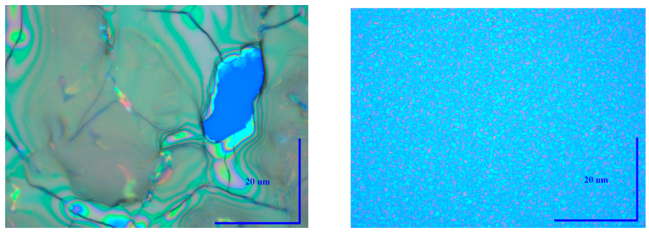

Figure 5. Optical microscopic image of (a) **2a** and (b) **2b** film on OTS-treated Si/SiO_2 after thermal annealing at 120 °C in vacuum for 1 h.

coated thin films of **2a** and **2b** annealed at 120 °C. It should be noted that the **2a** thin film exhibited a larger average grain size values than those of **2b** thin film, which can be interpreted by the better crystallinity of **2a** than that of **2b**. This can also explain why the OTFT device performance is better than that of **2b**. The observation is also confirmed by the AFM height images of **2a** and **2b** shown in Figure 6. It can be seen that the

crystal grain size of **2a** is beyond the range of the image, and is larger than those of **2b** (500−1000 nm).

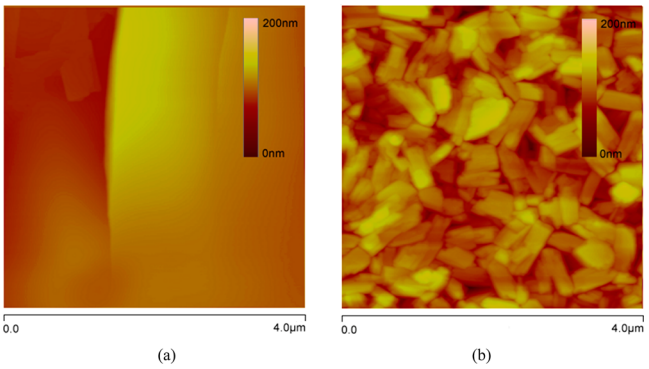

Figure 6. AFM height images of (a) **2a** (root mean square roughness: 9.31 nm) and (b) **2b** (root mean square roughness: 16.5 nm) film on OTS-treated Si/SiO_2 after thermal annealing at 120 °C in vacuum for 1 h.

5. Thin Film X-ray Diffraction (XRD). To get further information on the molecular order and orientations on the substrates, we carried out XRD experiments on the dip casting and spin-coating thin films in Figure 7. As shown in Figure 7a, for the films fabricated by the dip casting method, the **2a** film shows two broad peaks. In comparison, as shown in Figure 7b, when the films were fabricated by the spin-coating method and annealed at 120 °C, the broad peaks disappeared and a very sharp peak with very strong intensity at 2θ = 6.08 corresponding to the *d*-spacing of 14.5 Å is observed, indicating that crystallinity for **2a** films were obviously improved, thus the obvious increase of the electron mobility for **2a** devices. For **2b**, when the films were fabricated by dip-casting method shown in Figure 7a, a relatively sharp peak at 2θ = 4.04 corresponding to the *d*-spacing of 21.9 Å is observed compared with the broad peaks for **2a**, which indicated better crystallinity, thus resulting in higher electron mobility than those for **2a** under this condition. However, when the films were fabricated by spin-coating method and annealed at 120 °C shown in Figure 7b, the peak intensity is slightly increased. The phenomenon demonstrated the film crystallinity did not improve obviously under the two different conditions, thus a slight increase in electron mobilities for **2b.**

EXPERIMENTAL SECTION

Materials and Characterization. Melting points were obtained on a SHIMADZU DSC-60 instrument. 1H NMR spectra were recorded on a JEOL JNM-ECP300 NMR spectrometer, and chemical shifts were referenced to tetramethylsilane (TMS). Elemental analyses were carried out with a LECO/CHNS-932 analyzer (Chemical Resources Laboratory at the Tokyo Institute of Technology). EI mass spectra were collected on a JEOL JMS-700 mass spectrometer. UV−vis spectra were recorded on a SHIMADZU Multi Spec-1500 spectrometer. X-ray diffraction (XRD) was carried out in the reflection mode using a 2-kW Rigaku X-ray diffraction system. Atomic force microscopy (AFM) experiments were recorded on a Nanoscope V AFM in trapping mode.

Cyclic Voltammetry (CV) Measurements. Cyclic voltammetric measurements were carried out in a conventional three-electrode cell using a Pt disk working electrode, a platinum wire counter electrode, and a SCE reference electrode on a BAS-100B system at room temperature. Freshly distilled THF was used to prepare a solution of all compounds containing Bu_4NPF_6 (0.1 M) as supporting electrolyte. A ferrocenium/ferrocene couple ($E_{1/2}$= 0.46 V) was employed as the internal reference. The Pt disk working electrode was polished before each experiment with a 0.05 μm alumina paste, Ar bubbling was used to remove oxygen from the electrolyte solutions in the electrochemical cell.

Device Fabrication. An n-type heavily doped Si wafer with a SiO_2 layer of 300 nm and a capacitance of 11 nF cm^{-2} was used as the bottom gate electrode and dielectric layer. The thin films based on dip casting method of **2a** and **2b** were deposited on bare SiO_2/Si substrates using a 1 mg/mL chloroform solution. The thin films by spin-coating of **2a** and **2b** were deposited on octadecyltrichlorosilane (OTS)-treated substrates at a speed of 3000 rpm for 60 s using a 10 mg/mL chloroform solution. Next, the thin films were annealed at 120 °C in vacuum for 1 h to improve the film quality and morphology. Electrical measurements of OTFT devices were carried out at room temperature in air using a Hewlett-Packard 4140A and 4140B models or a Keithley 4200 semiconductor parameter analyzer. The mobilities were determined in the saturation regime by using the equation $I_{DS} = (\mu WC_i/2L)(V_G - V_T)^2$, where I_{DS} is the drain-source current, μ is the field-effect mobility, W is the channel width, L is the channel length, C_i is

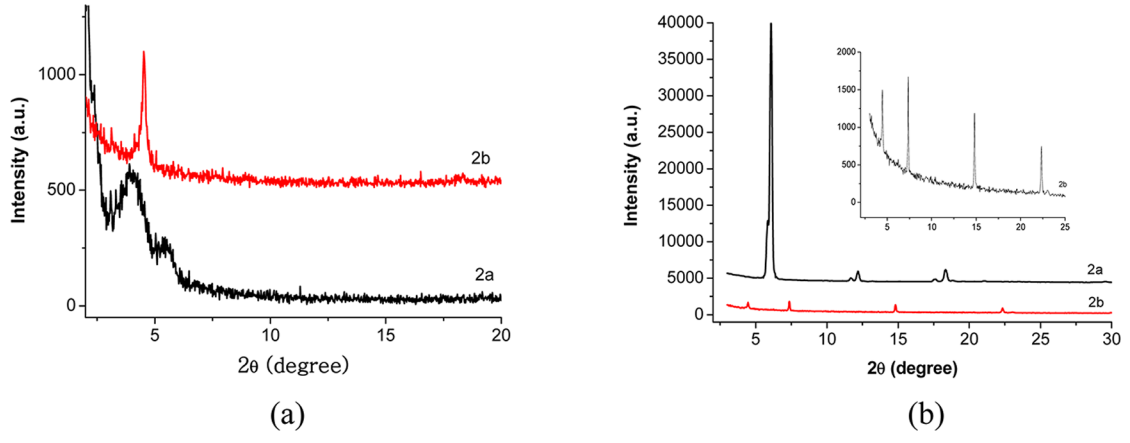

Figure 7. (a) XRD plots for films of **2a** and **2b** at room temperature deposited by dip casting, (b) XRD plots for films of **2a** and **2b** annealed at 120 °C deposited by spin-coating.

the capacitance per unit area of the gate dielectric layer, V_G is the gate voltage, and V_T is the threshold voltage.

2,3,6,7-Tetrabromo-4,8-dimethoxybenzo[1,2-*b*:4,5-*b*′]dithiophene. A solution of bromine (6.4 g, 40 mmol) in carbon disulfide (5 mL) was dropwise added to a solution of 4,8-dimethoxybenzo[1,2-*b*:4,5-*b*′]dithiophene (250 mg, 1.0 mmol) in carbon disulfide (15 mL), and the mixture was gently heated at reflux for 2 days. A saturated sodium hydrogensulfite aqueous solution was added to the resulting suspension. The precipitated solid was collected by filtration, washed with water and ethanol, and dried. A white solid (540 mg, 0.95 mmol) was obtained in a yield of 95%. For the insolubility of the compound in solvent, we cannot obtain its HNMR spectrum. MS: m/z 566 (M^+).

3,7-Dibromo-4,8-dimethoxybenzo[1,2-*b*:4,5-*b*′]dithiophene. Compound 2,3,6,7-tetrabromo-4,8-dimethoxybenzo[1,2-*b*:4,5-*b*′]dithiophene (566 mg, 1.0 mmol) was dissolved in acetic acid (100 mL) and heated at reflux, after which zinc dust (143 mg, 2.2 mol) was added in a potion to the solution. The resulting mixture was heated under reflux for 3 h. The mixture was then cooled to ambient temperature and diluted with water. The precipitate was filtered off, washed with water, dried, and purified by flash silica−l column chromatography using CH_2Cl_2: hexane = 1:2 as the eluent. A white solid (326 mg, 0.80 mmol) was obtained in 80% yield. MS: m/z 408 (M^+); ^{1}H NMR ($CDCl_3$, 300 MHz): 7.43 (s, 2H), 4.07 (s, 6H).

3,7-Di-(2-ethylhexyl)-4,8-dimethoxybenzo[1,2-*b*:4,5-*b*′]dithiophene. 3,7-Dibromo-4,8-dimethoxybenzo[1,2-*b*:4,5-*b*′]dithiophene (204 mg, 0.5 mmol) and [$NiCl_2$(dppp)] (27 mg, 0.05 mmol) were added to a separate three-necked round-bottom flask connected to a sintered glass filter. After purging with Ar, dry diethyl ether (50 mL) was added and the Grignard reagent (2-ethylhexyl)magnesium bromide (1.5 mL, 1 M in diethyl ether) was carefully added through the filter at room temperature. The reaction mixture was then refluxed for 12 h. After being cooled to room temperature, the mixture was quenched with 1N HCl. It was then filtered through a Celite bed and extracted with diethyl ether. The product was purified by flash silica-gel column chromatography using CH_2Cl_2: hexane = 1:4 as the eluent. A white solid (204 mg, 0.43 mmol) was obtained in 85% yield. MS: m/z 475 (M^+ + 1); ^{1}H NMR ($CDCl_3$, 300 MHz): 6.99 (s, 2H), 4.05 (s, 6H), 3.01 (t, 4H), 1.81−1.71 (m, 4H), 1.44−1.27 (m, 28H), 0.88 (t, 6H).

3,7-Didecyl-4,8-dimethoxybenzo[1,2-*b*:4,5-*b*′]dithiophene. The compound was prepared according to the same procedure as described for 3,7-di-(2-ethylhexyl)-4,8-dimethoxybenzo[1,2-*b*:4,5-*b*′]dithiophene. MS: m/z 532 (M^+ + 1); ^{1}H NMR ($CDCl_3$, 300 MHz): 6.99 (s, 2H), 2.91, 2.88 (d, 4H), 1.73−1.54 (m, 2H), 1.43−1.25 (m, 16H), 0.90 (t, 6H), 0.88 (t, 6H).

3,7-Di-(2-ethylhexyl)-2,6-dibromobenzo[1,2-*b*:4,5-*b*′]dithiophene-4,8-dione. A solution of bromine (0.8 g, 5 mmol) in CH_2Cl_2 (5 mL) was dropwise added to a solution of 3,7-di-(2-ethylhexyl)-4,8-dimethoxybenzo[1,2-*b*:4,5-*b*′]dithiophene (474 mg, 1.0 mmol) in CH_2Cl_2 (30 mL) and stirred for 2 h at room temperature. A saturated sodium hydrogensulfite aqueous solution was added to the solution to remove the excess of bromine, and extracted with CH_2Cl_2. The organic phase was washed with distilled water and dried over anhydrous Na_2SO_4. After the solvent was removed, the residue was purified by flash silica-gel column chromatography using CH_2Cl_2: hexane = 1:2 as the eluent. A yellow solid (566 mg, 0.94 mmol) was obtained in a yield of 94%. MS: m/z 601 (M^++1); ^{1}H NMR ($CDCl_3$, 300 MHz): 2.91, 2.88 (d, 4H), 1.73−1.54 (m, 2H), 1.46−1.23 (m, 16H), 0.90 (t, 6H), 0.88 (t, 6H).

3,7-Didecyl-2,6-dibromobenzo[1,2-*b*:4,5-*b*′]dithiophene-4,8-dione. The compound was prepared according to the same procedure as described for 3,7- di-(2-ethylhexyl)-2,6-dibromobenzo[1,2-*b*:4,5-*b*′]dithiophene-4,8-dione. MS: m/z 659 (M^+ + 1); ^{1}H NMR ($CDCl_3$, 300 MHz): 2.96 (t, 4H), 1.54−1.48 (m, 4H), 1.39−1.26 (m, 28H), 0.88 (t, 6H).

3,7-Di-(2-ethylhexyl)-2,6-trifluoromethylphenylbenzo[1,2-*b*:4,5-*b*′]dithiophene-4,8-dione. A mixture of 4-trifluoromethylphenylboronic acid (209 mg, 1.1 mmol), 3,7-di-(2-ethylhexyl)-2,6-dibromobenzo[1,2-*b*:4,5-*b*′]-dithiophene-4,8-dione (301 mg, 0.5 mmol) and $Pd(PPh_3)_4$ catalyst in 30 mL of 1 M aqueous K_2CO_3 solution and THF (v/v, 1:1) was heated at reflux for 24 h. After being cooled to room temperature, the mixture was extracted with of 100 mL of CH_2Cl_2 three times. The combined organic phase was washed with brine, dried over $MgSO_4$ and concentrated. The residue was purified by column chromatography using a mixture of CH_2Cl_2/hexane (1:1) as eluent to give the product as a yellow solid (334 mg, 0.456 mmol). Yield: 91%. .MS: m/z 732 (M^+); ^{1}H NMR ($CDCl_3$, 300 MHz): δ = 7.76, 7.74 (d, 4H), 7.59, 7.57 (d, 4H), 3.02−2.98 (t, 4H), 1.55 (s, 4H), 1.25−1.06 (m, 16H), 0.77 (t, 3H), 0.68 (t, 3H).

3,7-Didecyl-2,6-trifluoromethylphenylbenzo[1,2-*b*:4,5-*b*′]dithiophene-4,8-dione. The compound was prepared according to the same procedure as described for 3,7-di-(2-ethylhexyl)-2,6-trifluoromethylphenylbenzo[1,2-*b*:4,5-*b*′]-dithiophene-4,8-dione. MS: m/z 789 (M^++1); ^{1}H NMR ($CDCl_3$, 300 MHz): δ = 7.77, 7.74 (d, 4H), 7.60, 7.57 (d, 4H), 2.95 (t, 4H), 1.60−1.52 (m, 4H), 1.32−1.23 (m, 28H), 0.87 (t, 6H).

3,7- Di-(2-ethylhexyl)-2,6-trifluoromethylphenyl-4,8-dicyanoiminebenzo[1,2-*b*:4,5-*b*′]dithiophene (2a). To a stirred solution of the corresponding dione (**1a**) (366 mg, 0.5 mmol) (1 equiv) in dry chloroform was added titanium tetrachloride (10 equiv) followed by N,N-bis(trimethylsilyl)-carbodiimide (BTC) (10 equiv). The resulting dark solution was heated at reflux for 48 h. After cooling to room temperature, the solvent was removed in vacuo and the residue was purified by silica gel chromatography using a mixture of CH_2Cl_2/hexane (1:1) as eluent to afford a red solid **2a** (376 mg, 0.48 mmol) in a yield of 96%. MS: m/z 783 (M^++2); ^{1}H NMR ($CDCl_3$, 300 MHz): δ = 7.80, 7.77 (d, 4H), 7.61, 7.58 (d, 4H), 3.09−3.03 (m, 4H), 1.55 (s, 2H), 1.09−1.01 (m, 16H), 0.78 (t, 3H), 0.68 (t, 3H), Elemental anal. (%) Calcd for $C_{42}H_{42}F_6N_4S_2$: C, 64.60; H, 5.42; N, 7.17. Found: C, 64.65; H, 5.31; N, 7.14.

3,7-Didecyl-2,6-trifluoromethylphenyl-4,8-dicyanoiminebenzo[1,2-*b*:4,5-*b*′]dithiophene (2b). The compound was prepared according to the same procedure as described for 3,7- di-(2-ethylhexyl)-2,6-trifluoromethylphenyl-4,8-dicyanoiminebenzo[1,2-*b*:4,5-*b*′]dithiophene. MS: m/z 838 (M^++1); ^{1}H NMR ($CDCl_3$, 300 MHz): δ = 7.78, 7.81 (d, 4H), 7.63, 7.60 (d, 4H), 2.99 (t, 4H), 1.55 (m, 4H), 1.29−1.24 (m, 28H), 0.88 (t, 6H), Elemental anal. (%) Calcd for $C_{46}H_{50}F_6N_4S_2$: C, 66.01; H, 6.02; N, 6.69. Found: C, 66.15; H, 6.02; N, 6.69.

CONCLUSIONS

In summary, two new benzodithiophene derivatives as solution-processed n-type semiconductors have been successfully synthesized and characterized. Different long alkyl group substituents affect the arrangement and the crystallinity of the molecules in the solid state, which is revealed by the UV−vis spectroscopy, XRD, AFM and the OTFT performances. Because of the better arrangement of molecules and the good crystallinity, a very air-stable device for **2a** film was fabricated by the spin-coating method which showed the highest mobility 0.003 $cm^2 V^{-1} s^{-1}$ with on/off of 1×10^5. Further studies such as optimizing molecular architectures and devices characteristics are currently underway.

ASSOCIATED CONTENT

Supporting Information

^1H NMR spectra of the synthesized compounds. This material is available free of charge via the Internet at http://pubs.acs.org.

AUTHOR INFORMATION

Corresponding Author

*E-mail: chensy@dhu.edu.cn; yoshiro@echem.titech.ac.jp.

Notes

The authors declare no competing financial interest.

ACKNOWLEDGMENTS

This work is supported by a Grant-in-Aid for Scientific Research (19350092 and 22550162) from the Ministry of Education, Culture, by Sports, Science and Technology, Japan, by the Global COE program "Education and Research Center for Emergence of New Molecular Chemistry", by Doctoral Fund of Ministry of Education of China (20090075120011), and The National Natural Science Foundation of China (51003012). S.C. expresses her sincere thanks to the JSPS for a postdoctoral fellowship for foreign researchers (P09255).

REFERENCES

(1) Wen, Y.; Liu, Y *Adv. Mater.* **2010**, *22*, 1331.
(2) Murphy, A. R.; Fréchet, J. M. J. *Chem. Rev.* **2007**, *107*, 1066.
(3) Zaumseil, J.; Sirringhaus, H. *Chem. Rev.* **2007**, *107*, 1296.
(4) Mas-Torrent, M.; Rovira, C. *Chem. Soc. Rev.* **2008**, *37*, 827.
(5) Park, Y. D.; Lim, J. A.; Lee, H. S.; Cho, K. *Mater. Today* **2007**, *10*, 46.
(6) Coropceanu, V.; Cornil, J.; da Silva Filho, D. A.; Olivier, Y.; Silbey, R.; Brédas, J.-L. *Chem. Rev.* **2007**, *107*, 926.
(7) Afzali, A.; Dimitrakopoulos, C. D.; Breen, T. L. *J. Am. Chem. Soc.* **2002**, *124*, 8812.
(8) Payne, M. M.; Parkin, S. R.; Anthony, J. E.; Kuo, C. C.; Jackson, T. N. *J. Am. Chem. Soc.* **2005**, *127*, 4986.
(9) Li, Y.; Singh, S. P.; Sonar, P. *Adv. Mater.* **2010**, *22*, 4862.
(10) Li, Y.; Sonar, P.; Singh, S. P.; Soh, M. S.; van Meurs, M.; Tan, J. *J. Am. Chem. Soc.* **2011**, *133*, 2198.
(11) Ha, J. S.; Kim, K. H.; Choi, D. H. *J. Am. Chem. Soc.* **2011**, *133*, 10364.
(12) Gao, X.; Di, C.; Hu, Y.; Yang, X.; Fan, H.; Zhang, F.; Liu, Y.; Li, H.; Zhu, D. *J. Am. Chem. Soc.* **2010**, *132*, 3697.
(13) Hu, Y.; Gao, X.; Di, C.; Yang, X.; Zhang, F.; Liu, Y.; Li, H.; Zhu, D. *Chem. Mater.* **2011**, *23*, 1204.
(14) Zhao, Y.; Di, C.; Gao, X.; Hu, Y.; Guo, Y.; Zhang, L.; Liu, Y.; Wang, J.; Hu, W.; Zhu, D. *Adv. Mater.* **2011**, *23*, 2448.
(15) Wu, Q.; Li, R.; Hong, W.; Li, H.; Gao, X.; Zhu, D. *Chem. Mater.* **2011**, *23*, 3138.
(16) Polander, L. E.; Tiwari, S. P.; Pandey, L.; Seifried, B. M.; Zhang, Q.; Barlow, S.; Risko, C.; Brédas, J.-L.; Kippelen, B.; Marder, S. R. *Chem. Mater.* **2011**, *23*, 3408.
(17) Usta, h.; Facchetti, A.; Marks, T. B. *Acc. Chem. Res.* **2011**, *44*, 501.
(18) Yan, H.; Chen, Z. H.; Zheng, Y.; Newman, C.; Quinn, J. R.; Dotz, F.; Kastler, M.; Facchetti, A. *Nature* **2009**, *457*, 679.
(19) Jones, B. A.; Facchetti, A.; Wasielewski, M. R.; Marks, T. J. *J. Am. Chem. Soc.* **2007**, *129*, 15259.
(20) Yan, H.; Zheng, Y.; Blache, R.; Newman, C.; Lu, S.; Woerle, J.; Facchetti, A. *Adv. Mater.* **2008**, *20*, 3393.
(21) Chen, Z.; Zheng, Y.; Yan, H.; Facchetti, A. *J. Am. Chem. Soc.* **2009**, *131*, 8.
(22) Sista, P.; Biewer, M. C; Stefan, M. C. *Macromol. Rapid Commun.* **2012**, *33*, 9.
(23) Mamada, M.; Kumaki, D.; Nishida, J.; Tokito, S.; Yamashita, Y. *ACS Appl. Mater. Interfaces* **2010**, *2*, 1303.
(24) Pan, H.; Li, Y.; Wu, Y.; Liu, P.; Ong, B. S.; Zhu, S.; Xu, G. *J. Am. Chem. Soc.* **2007**, *129*, 4112.
(25) Takimiya, K.; Kunugi, Y.; Konda, Y.; Niihara, N.; Otsubo, T. *J. Am. Chem. Soc.* **2004**, *126*, 5084.
(26) Pan, H.; Li, Y.; Wu, Y.; Liu, P.; Ong, B. S.; Zhu, S.; Xu, G. *Chem. Mater.* **2006**, *18*, 3237.
(27) Zhao, X.; Zhan, X. *Chem. Soc. Rev.* **2011**, *40*, 3728.
(28) Price, S. C.; Stuart, A. C.; Yang, L.; Zhou, H.; You, W. *J. Am. Chem. Soc.* **2011**, *133*, 4625.
(29) Hou, J.; Chen, H.-Y.; Zhang, S.; Chen, R. I.; Yang, Y.; Wu, Y.; Li, G. *J. Am. Chem. Soc.* **2009**, *131*, 15586.
(30) Huo, L.; Hou, J.; Zhang, S.; Chen, H.-Y.; Yang, Y. *Angew. Chem., Int. Ed.* **2010**, *49*, 1500.
(31) Huo, L.; Guo, X.; Zhang, S.; Li, Y.; Hou, J. *Macromolecules* **2011**, *44*, 4035.
(32) Wang, M.; Hu, X.; Liu, P.; Li, W.; Gong, X.; Huang, F.; Cao, Y. *J. Am. Chem. Soc.* **2011**, *133*, 9638.
(33) Jiang, J.-M.; Yang, P.-A.; Chen, H.-C.; Wei, K.-H. *Chem. Commun.* **2011**, *47*, 8877.
(34) Hünig, S. *J. Mater. Chem.* **1995**, *5*, 1469.
(35) Takahashi, K.; Mazaki, Y.; Kobayashi, K. *Chem. Commun.* **1996**, 2275.
(36) Takahashi, K.; Kobayashi, K. *J. Org. Chem.* **2000**, *65*, 2577.
(37) de la Cruz, P.; Mart, N.; Miguel, F.; Seoane, C. *J. Org. Chem.* **1996**, *61*, 6192.
(38) Shiraishi, K.; Yamamoto, T. *Polym. J.* **2002**, *34*, 727.
(39) Batsanov, A. S.; Bryce, M. R.; Coffin, M. A.; Green, A.; Hester, R. E.; Howard, J. A. K.; Lednev, I. K.; Martín, N.; Moore, A. J.; Moore, J. N.; Ortí, E.; Sánchez, L.; Savirón, M.; Viruela, P. M.; Viruela, R.; Ye, T.-Q. *Chem.—Eur. J.* **1998**, *4*, 2580.
(40) Ribierre, J. C.; Fujihara, T.; Watanabe, S.; Matsumoto, M.; Muto, T.; Nakao, A.; Aoyama, T. *Adv. Mater.* **2010**, *22*, 1722.
(41) Ribierre, J. C.; Aoyama, T.; Watanabe, S.; Gu, J.; Muto, T.; Matsumoto, M.; Nakao, A.; Wada, T. *Jpn. J. Appl. Phys.* **2010**, *49*, 01AB06.
(42) Ribierre, J.-C.; Watanabe, S.; Matsumoto, M.; Muto, T.; Nakao, A.; Aoyama, T. *Adv. Mater.* **2010**, *22*, 4044.
(43) Ie, Y.; Nishida, K.; Karakawa, M.; Tada, H.; Asano, A.; Saeki, A.; Seki, S.; Aso, Y. *Chem.—Eur. J.* **2011**, *17*, 4750.
(44) Usta, H.; Risko, C.; Wang, Z.; Huang, H.; Deliomeroglu, M. K.; Zhukhovitskiy, A.; Facchetti, A.; Marks, T. J. *J. Am. Chem. Soc.* **2009**, *131*, 5586.
(45) de Leeuw, D. M.; Simenon, M. M. J.; Brown, A. R.; Einerhand, R. E. F. *Synth. Met.* **1997**, *87*, 53.
(46) Anthopoulos, T. D.; Anyfantis, G. C.; Papavassiliou, G. C.; de Leeuw, D. M. *Appl. Phys. Lett.* **2007**, *90*, 122105.